Comparison of the lifting-line free vortex wake method and the blade-element-momentum theory regarding the simulated loads of multi-MW wind turbines

S. Hauptmann[1], M. Bülk[1], L. Schön[2], S. Erbslöh[2], K. Boorsma[3], F. Grasso[3], M. Kühn[4], P. W. Cheng[1]

[1] Stuttgart Wind Energy, Universität Stuttgart, Stuttgart, Germany
[2] REpower Systems SE, Osterrönfeld, Germany
[3] Energy Research Centre of the Netherlands (ECN), Petten, The Netherlands
[4] ForWind – Universität Oldenburg, Oldenburg, Germany

E-mail: hauptmann@ifb.uni-stuttgart.de

Abstract. Design load simulations for wind turbines are traditionally based on the blade-element-momentum theory (BEM). The BEM approach is derived from a simplified representation of the rotor aerodynamics and several semi-empirical correction models. A more sophisticated approach to account for the complex flow phenomena on wind turbine rotors can be found in the lifting-line free vortex wake method. This approach is based on a more physics based representation, especially for global flow effects. This theory relies on empirical correction models only for the local flow effects, which are associated with the boundary layer of the rotor blades. In this paper the lifting-line free vortex wake method is compared to a state-of-the-art BEM formulation with regard to aerodynamic and aeroelastic load simulations of the 5MW UpWind reference wind turbine. Different aerodynamic load situations as well as standardised design load cases that are sensitive to the aeroelastic modelling are evaluated in detail. This benchmark makes use of the AeroModule developed by ECN, which has been coupled to the multibody simulation code SIMPACK.

1. Introduction

The design and certification of modern wind turbines is based on a set of so called design load cases (DLC´s). Such DLC´s are defined by e.g. the International Electrotechnical Commission (IEC) [1] or the Germanischer Lloyd (GL) [2]. The design load cases represent all situations that a wind turbine is expected to be exposed to in its design life time. To simulate a DLC, the wind turbine structure has to be simulated as well as its interaction with the external loads. The complex interaction of the wind turbine with the external wind field is described by the rotor aerodynamics and the aeroelasticity. Traditionally, the rotor aerodynamics is simulated by applying the blade-element-momentum theory (BEM). The BEM approach is based on simplified physics. To achieve an acceptable accuracy for the prediction of the rotor loads anyhow, several semi-empirical correction models have been developed. To account for the aeroelastic effects, the structure of the wind turbine is represented by the relevant structural degrees of freedom to model the low frequent wind turbine structural dynamics [1]. This approach has been applied for the wind turbine design process for decades and is still the industry standard. Nevertheless, the significance of this approach for modern wind turbines is questionable. The design of large, optimized modern wind turbines relies on an accurate prediction of the

dimensioning loads. Complex turbine conditions that result in non-uniform induction like e.g. yawed inflow, pitch asymmetry, or heavily deflected rotor blades violate the assumptions of BEM and its correction models. In the last years more advanced aerodynamic approaches have been developed and are available for the aeroelastic load simulations of wind turbines. A more sophisticated but still computationally efficient approach to account for the complex flow phenomena on wind turbine rotors can be found in the lifting-line theory in combination with a free vortex wake method. This approach is based on a more physics based representation, especially for stationary and non-stationary global flow effects that are related to dynamic wake effects. This theory relies on empirical correction models only for the local flow effects, which are associated with the boundary layer of the rotor blades.

This paper evaluates in detail how the lifting-line free vortex wake method (FVM) can be used for a more accurate load determination compared to a modern BEM formulation for a large generic wind turbine. This benchmark makes use of the AeroModule developed by ECN [3] that offers both an advanced BEM formulation and a variant of the lifting-line FVM method, named AWSM [4]. Both aerodynamic approaches have been extensively validated against wind tunnel experiments using the NASA-AMES [5] and MEXICO [6] wind tunnel test databases. The AeroModule is coupled to the multibody simulation software package SIMPACK that is used to simulate the structural dynamics of the wind turbine. All simulations are based on the 5MW UpWind reference wind turbine with a rotor diameter of 126m and a rated rotor speed of 12.1 rpm [7].

The paper is divided into five chapters. The introduction is followed by a text section that discusses the basic theory of the two different aerodynamic models that are considered. In the third part, specific aerodynamic situations are evaluated with the different models are described, while the fourth chapter analyses the impact of the FVM and the BEM approach on exemplary design load cases. In the last part the paper ends with a conclusion.

2. Theory of the aerodynamic models used

A detailed description of the BEM approach within the ECN AeroModule can be found in [3] and the derivation of the lifting-line FVM is given in [4]. Both approaches have their own assumptions, advances and shortcomings. These are discussed in the current section.

2.1. The BEM method

The BEM approach relates the axial and tangential momentum equations for a stream tube (annulus) to the local blade forces. These equations are solved iteratively, yielding the rotor induced velocities in axial and tangential direction. The following assumptions are made when deriving a typical BEM formulation, i.e. for the ECN AeroModule:

- The rotor plane is sliced into annuli with no radial dependence and radial induction.
- The force on each annular element is constant over the circumference of the annulus.
- The momentum is always balanced in planes parallel to the rotor disc and the rotor blades are assumed being in the rotor plane.
- The flow field around the rotor is always in equilibrium, without any time delay.
- The airfoil characteristics can be determined beforehand in 2D measurements or simulations.

Several engineering extensions exist to account for the shortcomings of this approach. [3]

2.1.1. Tip and root loss correction. To account for the finite number of blades, the empirical Prandtl correction [8] for the root and the tip is calculated for each element. Root and tip loss factors are multiplied to result in a ’total’ Prandtl factor. The Prandtl factor then relates the annulus averaged axial and tangential induction to the local induction at each element.

2.1.2. Oblique inflow correction. The rotor plane is often angled with respect to the incoming wind field during turbine operation, resulting in conditions different from axial flow. These conditions can arise due to wind direction variation or a tilted rotor, which are subsumed under an effective yaw angle. One effect of the oblique inflow arises due to an azimuthal variation of the wind velocity that is

experienced by an element during a rotor revolution. This advancing and retreating blade effect is implicitly included in the velocities coming from the wind and the structure motions. To account for the variation of axial induction within each annulus, a model as defined by Schepers [9, 10] is employed which is based on [21]. A skew function f_{skew} is determined for each element as a function of effective yaw angle, azimuth angle and radial location. This skew function then relates the local induction at each element to the annulus averaged axial induction.

2.1.3. Dynamic inflow model. The dynamic inflow model used in the AeroModule has been developed by ECN [11]. The model adds another term to the axial momentum equation to account for the inertia of the flow stream that interacts with the rotor in the case of pitch action, rotational speed variation or wind speed variation. The term is proportional to the time derivative of the annulus averaged axial rotor induction and has a dependency on the radial position. Amongst others, this model has been validated against measurements in EU-sponsored projects [11].

2.1.4. Turbulent wake state model. For heavily loaded rotors, BEM theory predicts flow reversal in the wake, whilst in reality the wake transforms into a turbulent state by sucking in air from outside the stream tube [20]. To account for this effect the momentum equation is replaced by a turbulent wake state equation if the annulus averaged axial induction coefficient exceeds a user specified value. The default value for this parameter is 0.38. The quadratic relationship between axial force and induction in the momentum equation is then replaced by a linear relationship tangent to the original quadratic line at the specified induction value [3].

2.1.5. Stall delay model. The 3D correction model as developed by Snel [12] to account for the effects of rotation on the airfoil coefficients has been implemented.

2.1.6. Dynamic stall models. Dynamic stall models account for the fact that the local state at each airfoil section is not able to respond instantaneously to changing conditions like turbulence, blade deformation or tower effects. Especially for separated flow conditions, the dynamic value of the airfoil coefficients will differ from the static look-up value. The Snel first order [13] and alternatively the Snel second order [13] models are available. Dynamic effects for attached flow in the form of a modified Theodorsen model [14] will be implemented in future [15].

2.2. The lifting-line free vortex wake method (AWSM)

The AWSM code [4], representing the lifting-line FVM in the ECN AeroModule applies the potential flow theory that is mathematically based on Laplace's equation to describe the flow field at the blades as well as in the wake. Wake-induced velocities are obtained through evaluation of the Biot-Savart law. The mathematical approach to calculate the actual lift on a blade element due to the induced velocities is given by the Kutta-Joukowski equation. These equations are solved iteratively, yielding the induced velocities locally at each blade section, depending on the wake. The induced velocities are calculated for all spatial directions leading to the local axial, tangential and radial induction. The following assumptions are made when deriving the formulation for AWSM:

- In each section, the lift generated by a lifting surface, acts at the quarter chord location.
- The expansion in spanwise direction is predominant compared to the chord and thickness.
- Inviscid flow is assumed. The effects of viscosity are taken into account through the nonlinear relationship between local flow direction and local lift, drag and pitching moment coefficients.
- Locally occurring onset flow velocities are supposed to be much smaller than the speed of sound and therefore incompressible flow can be assumed.
- Only vorticity effects are modeled. Thickness or displacement effects are not included.
- The potential theory assumes irrotational flow.
- The airfoil characteristics can be determined beforehand in 2D measurements or simulations.

Most of the assumptions are valid for a wind turbine rotor. The assumption of inviscid flow and the reliance on airfoil tables is discussed in Chapter 2.3. The assumption of irrotational flow is not valid for the entire potential flow field as described in Chapter 2.2.1.

2.2.1. Vortex core models. When approaching the vortex line itself for an evaluation point, the Bio-Savart law behaves singularly. This is circumvented in AWSM with the introduction of a vortex core model depending on a user-specific cut-off radius [4]. This cut-off can be chosen as smooth or linear within AWSM.

2.3. Comparison of the assumptions of BEM and the lifting-line FVM

The aerodynamic situations that are relevant for the wind turbine rotor can be related to either global or local flow effects and can be stationary or non-stationary. The global flow effects are related mainly to the interaction of the blade section with the wake and the overall rotor induction, while the local flow effects are associated with the flow in the boundary layer on the blade. The global flow effects that are captured by engineering models in BEM can be physically solved with the lifting-line FVM method. Engineering models for the local effects are considered by both the BEM and the lifting-line FVM approach. Table 1 shows an overview about all relevant aerodynamic situations.

Table 1: Classification of the aerodynamic situations

Aerodynamic situation	**Classification**	**Consideration BEM**	**Consideration AWSM**
Axial induction	Global / stationary	Intrinsic	Intrinsic
Tangential induction	Global / stationary	Intrinsic	Intrinsic
Radial induction	Global / stationary	Not included	Intrinsic
Finite number of blades	Global / stationary	Engineering model	Intrinsic
Oblique inflow	Global / stationary	Engineering model	Intrinsic
Turbulent wake state	Global / stationary	Engineering model	Intrinsic
Dynamic inflow	Global / non-stat.	Engineering model	Intrinsic
Stall delay	Local / stationary	Engineering model	Engineering model
Dynamic stall	Local / non-stat.	Engineering model	Engineering model

Since the local effects have to be considered by engineering models as well in BEM as in AWSM, only the global aerodynamic effects are evaluated in detail in the paragraphs below. More advanced methods to analyse the local effects in detail can be found e.g. in [16].

3. Aerodynamic situations

As shown in Chapter 2, AWSM offers a more physical approach compared to BEM, especially for aerodynamic effects that are related to the global flow field. To analyze the advantages of AWSM, aerodynamic situations are evaluated using BEM and AWSM at the instance of the 5MW UpWind reference wind turbine. The selected situations are both relevant for the design load cases and sensitive to the aerodynamic modeling. The turbine structure is modeled rigid, with a fixed rotor speed to put the focus on the aerodynamics.

3.1. Reference situation

The reference situation describes an idealized turbine. The rotor is not yawed, and the blades are not coned, tilted or pitched. The rotor is operating at the optimal tip speed ratio with a wind speed of $v = 8$ m/s and a fixed rotational speed of $\Omega = 9.155$ rpm. All blade elements align with the rotor plane and the inflow is perpendicular to this plane. This situation is in accordance with almost all assumptions made in the BEM approach; only the correction model for tip and root loss must be applied. AWSM does not apply any corrections for this situation.

From Fig. 1 the out-of-plane blade root bending moment as predicted by BEM and AWSM as a function of time can be seen. The AWSM code needs some time to reach a steady-state condition

because the wake has to develop. For all further situations and load cases, care has been taken that the evaluation is not distorted by any initial transient effects. After reaching a steady state condition, the simulated bending moments as predicted by both codes do fit together like expected.

Fig. 2 illustrates the angle of attack over the blade length for the last simulated time step. A very good agreement of both aerodynamic approaches can be observed. The maximum predicted difference is in the order of 0.1 deg which is neglectable.

To analyze the prediction of the tip and root losses of the BEM approach in detail, the Prandtl factor is evaluated. The Prandtl factor relates the annulus averaged axial and tangential induction to the local induction at each blade element. In the BEM approach the annulus averaged induction is calculated and the engineering model that accounts for the tip and root losses calculates the Prandtl factor. For the calculation of the angle of attack, the local induction as a result of the application of the Prandtl factor on the annulus averaged induction is used. In AWSM, the local induction is a direct result of the applied method. To calculate the Prandtl factor, the annulus averaged induction has to be determined. This is done using the reduced axial velocity method, described by Hansen [17].

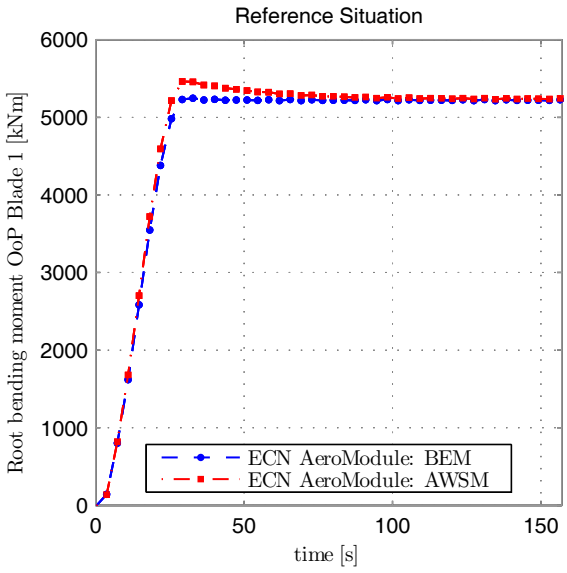

Fig. 1: Blade 1 out-of-plane bending moment as predicted by BEM and AWSM over time

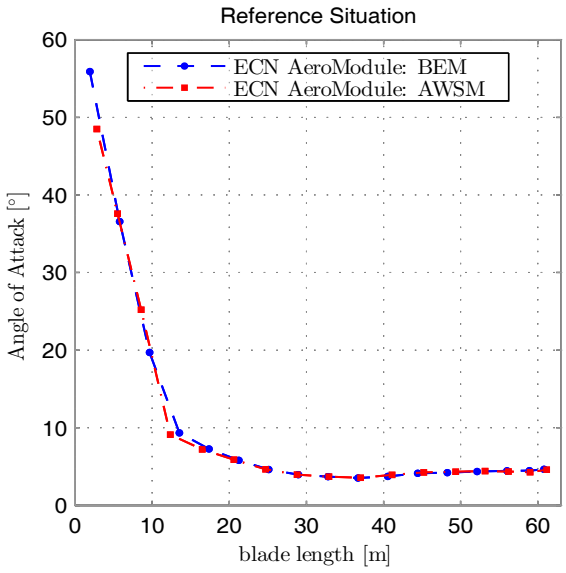

Fig. 2: Angle of attack over blade length at t=157.4 s

Figures 3 and 4 highlight the simulated local and annulus averaged axial induction factors and the corresponding Prandtl factors using both aerodynamic approaches. Apart from the root section where numerical problems occur applying the reduced axial velocity method, a good agreement in the induction factors is found. This correlation of the tip and root losses has been confirmed for the reference situation only. One can expect diverging results in the tip and root prediction for different conditions. Other publications deal with this topic [18, 19], seeing a high potential in the lifting-line approach for accurate tip and root loss prediction.

Since the local wind velocities and the local angles of attack show a very good agreement, the local loads that are derived from those variables are also expected to coincide. This has been verified.

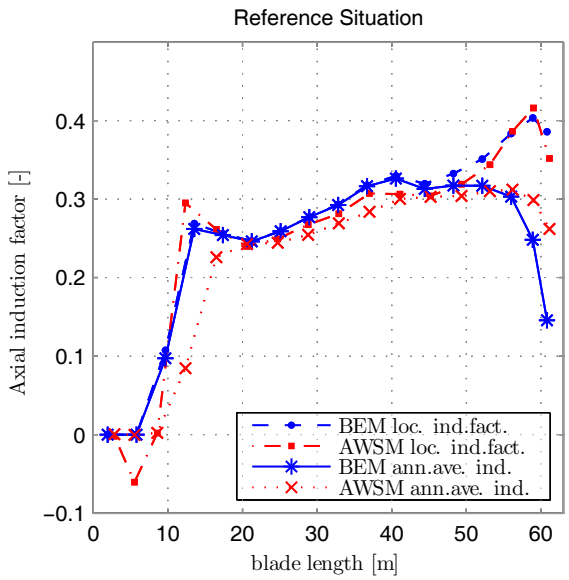

Fig. 3: Local and annulus averaged axial induction factors as predicted by BEM and AWSM

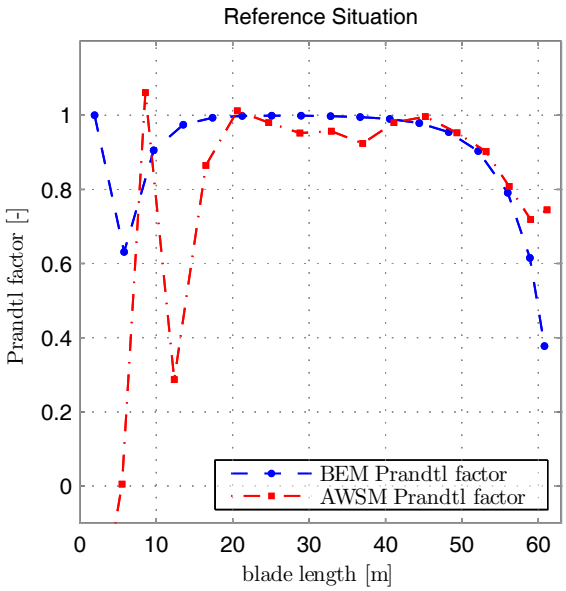

Fig. 4: The resulting Prandtl factor as predicted by AWSM and BEM

3.2. Cone situation

The BEM approach assumes that the rotor blades are aligned with the rotor plane. This is often not the case since the blades are deflected out of the rotor plane for various reasons. It is obvious that the blades bend in downwind direction when loaded. To increase the tower clearance, the rotor blades are sometimes pre-bended or mounted with a cone angle to deflect in upwind direction. To analyse this effect, the rigid rotor as defined in the reference situation is modified by a cone angle of -2.5 deg that deflects the blades in upwind direction. The wind speed of v = 8 m/s and the rotational speed of Ω = 9.155 rpm coincide with the reference situation. To describe the effect of coning, Figure 5 shows the axial, tangential and radial induction in the rotor plane as predicted with AWSM in the reference case. The axial and tangential induction is also covered with the BEM approach, while the radial induction is not. The radial induction is caused by the expansion of the stream tube. As shown in Figure 5, the radial expansion of the stream tube is directed towards low axial induction. Therefore, the radial induction in the outer part is directed radially outwards, while in the inner part, the radial induction is directed to the hub center. In the reference case this radial induction has no influence on the angle of attack and the loads because the radial induction acts along the blades. In the cone situation the radial induction has a component perpendicular to the blade span and therefore a load variation can be expected.

Figure 6 shows the radial induced velocity as a function of the rotor radius for the reference load situation compared to the coned load situation. The wind speed and rotational speed has not been modified. It is shown that the radial induction is negative between the hub center and a radius of 20 m and positive elsewhere and the cone angle does only have a minor influence on the result. Figure 7 illustrates the angle of attack over the rotor radius as predicted by BEM and AWSM for the coned case as well as for the reference case. The angle of attack that is predicted by BEM is the same for the reference case and the coned case. The angle of attack as predicted by AWSM does vary due to the cone angle. The radial position that shows a negative radial induction shows a lower angle of attack for the coned case compared to the reference case and vice versa as expected. Since the cone angle in this situation is quite large and the magnitude of the change in angle of attack is insignificant, the described effect is negligible within the design process.

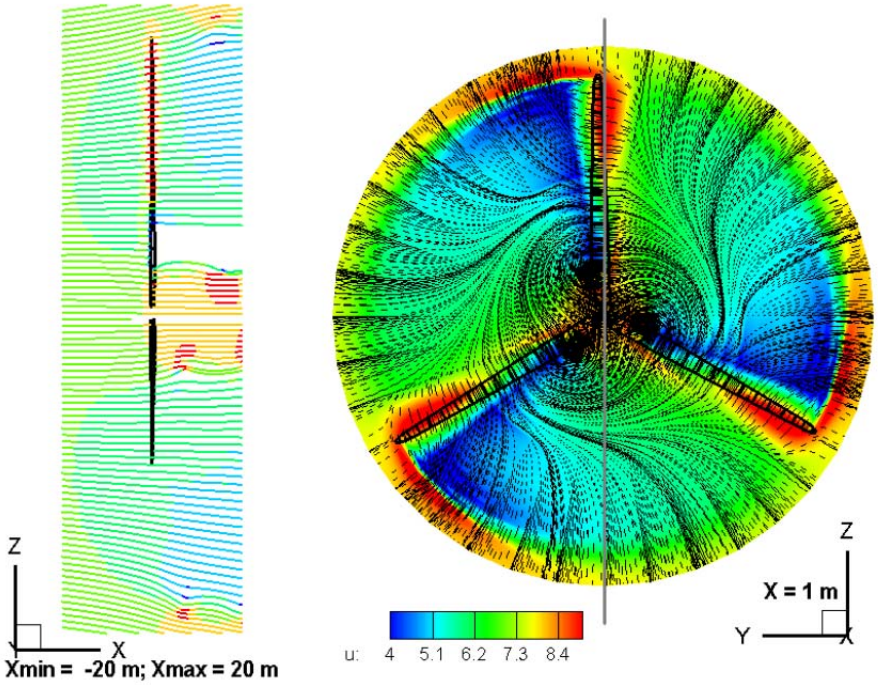

Fig. 5: Stream traces – radial and tangential induction in rotor plane

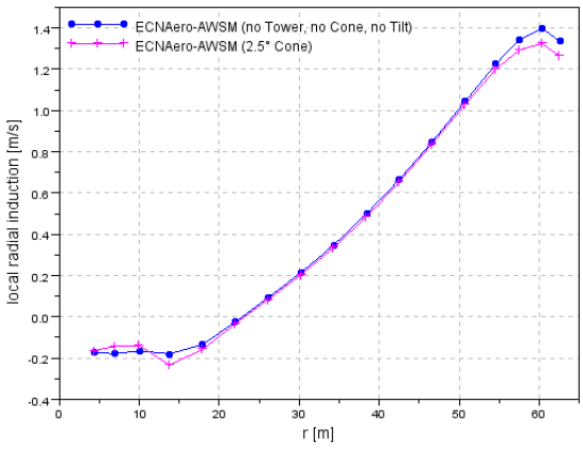

Fig. 6: Radial induction over r for reference and cone situation

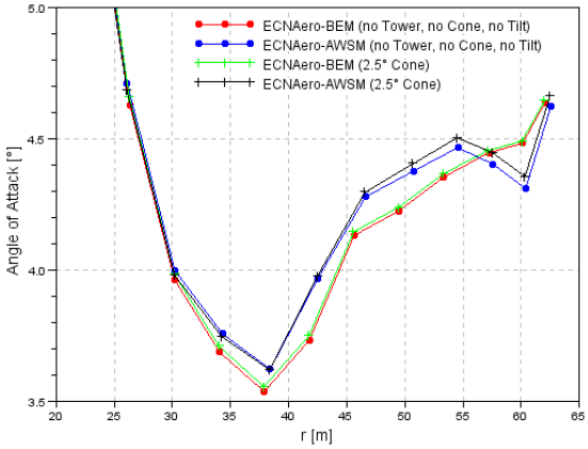

Fig. 7: Angle of attack over rotor radius r

3.3. Oblique inflow situation

As described in Chapter 2, the oblique inflow results in two different effects that have to be considered in the aerodynamic simulations. The advancing and retreating blade effect occurs due to the blade motion through the angled incoming wind field. This effect is implicitly included in both aerodynamic methods that are evaluated. The second effect is the skewed wake effect. This effect is implicitly included in the lifting-line FVM method, but the BEM approach relies on an engineering model to account for this effect.

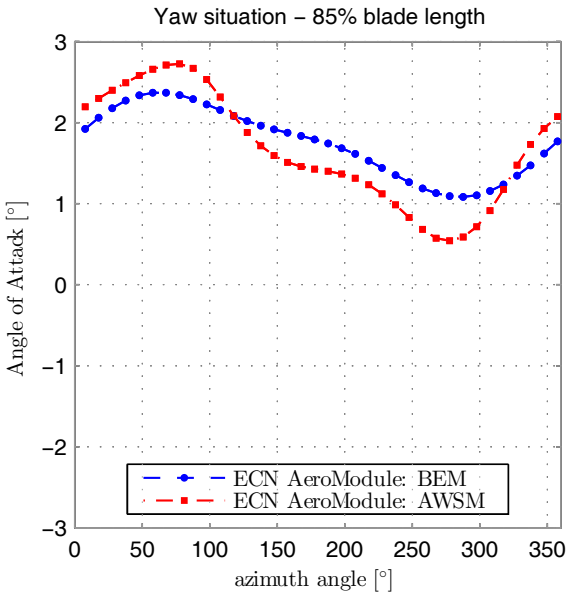

Fig.8: Angle of attack at 85% span over the azimuth angle in case of a 60 deg yaw angle

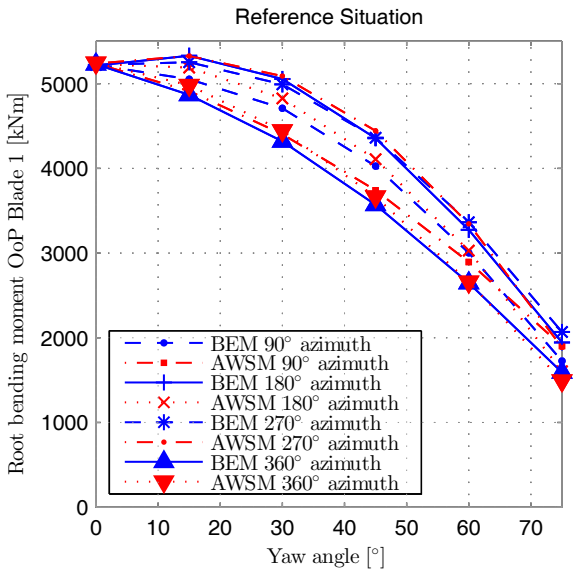

Fig. 9: Blade 1 out-of-plane bending moment over yaw angle for various azimuth angles

In Figure 8, the angle of attack for one rotor blade at a position of 85% span is drawn over the azimuth angle for a yaw angle of 60 deg. The trends of the angles of attack derived with BEM and AWSM are comparable, indicating the advanced engineering model in BEM. Nevertheless, the differences, especially at the azimuthal positions close to 90 deg and 270 deg cannot be neglected and could lead to differing loads in the design load cases. The blade 1 out-of-plane bending moment over the yaw angle for various azimuth angles as presented in Figure 9 confirms this estimation.

3.4. Individual pitch situation

The individual pitch situation is used to evaluate the dynamic inflow model of BEM and the interdependency of all three rotor blades due to the wake. BEM cannot model this interdependency as this approach makes use of annulus averaged induction. AWSM, however, intrinsically accounts for all effects that arise from the individual pitch maneuvre. The time history of the vortices in the wake of the individual blades influences the induction in the rotor plane.

After reaching steady state conditions, an individual pitch maneuvre of blade 1 is executed from 0 deg to 3 deg towards feather with a rate of 8 deg/s. The pitch angles 2 and 3 remain at 0 deg.

The effects covered by the different methods result in diverging angles of attack. After the rapid decrease of the angle of attack, an inconsistency between the AWSM and BEM results is visible in Figure 10. This is caused by the empirical dynamic inflow model in BEM that accounts for the individual pitch action as a uniform change of induction at all three blades simultaneously. Hence, BEM predicts the same change in angle of attack for blade 2 and 3 (Not shown in the figure). In contrast to the BEM calculation, AWSM takes the interdependency of all three blades into account by modelling their individual wakes and their mutual interaction as seen in Figure 11. The magnitude of the difference in the angles of attack for all three blades indicates that such an individual pitch situation in a design load case could result in differing loads as predicted by AWSM in contrast to BEM.

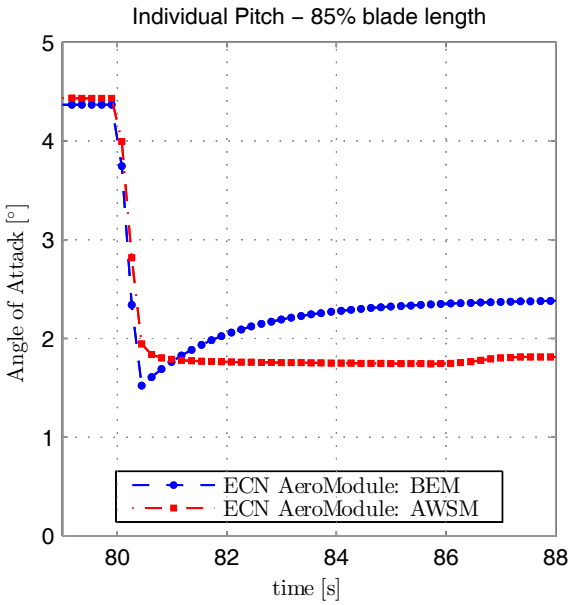

Fig.10: Angle of attack at 85% span over time for an individual pitch action

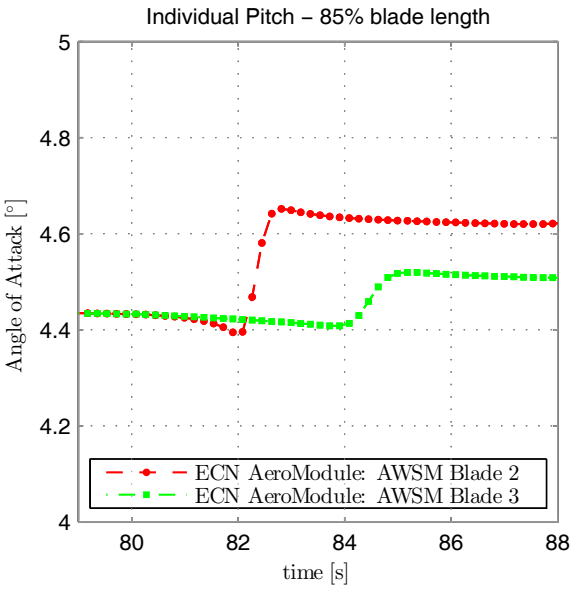

Fig. 11: AWSM: Angle of attack of blades 2 & 3 for an individual pitch action on blade 1

4. Design Load Cases

A more accurate prediction of the global effects that are related to the rotor aerodynamics has been demonstrated for AWSM compared to BEM in the last paragraph. To evaluate the relevance of increased accuracy for the design process, the aerodynamically sensitive DLC´s as defined by IEC are evaluated with both aerodynamic approaches. For the simulations of the DLC´s the structural dynamics and the aeroelasticity are taken into account as a flexible multibody model which is presented in [7].

The quality of AWSM becomes relevant especially for non-uniform induction within the rotor plane. Individual pitch maneuvers have already been identified to cause such an effect. Modern wind turbines are often equipped with independent pitch actuators, so that the three rotor blades can be used as independent aerodynamic brakes. In case of a malfunction of one pitch system, pitching of the remaining blades brings the turbine into a safe parked or idling condition. The quantification of the loads acting on the turbine in the case of such an event is described in IEC DLC 2.1.

Another load case that results in a non-uniform induction over the rotor disc is the IEC DLC 1.4. This design load case covers extreme wind events. In this load case an extreme coherent gust occurs with a simultaneous change of the wind direction while the turbine is producing power.

4.1. IEC DLC 2.1 - Pitch system fault

The fault condition occurs when the turbine is in power production mode. The control system reacts on the fault and brings the turbine into a safe condition. This situation has to be verified for any wind speed between cut-in and cut-off wind speed. In this paper the load case is slightly modified: The incoming wind speed is defined as a “normal wind profile” as demanded by the GL guideline in contrast to the “normal turbulence model” that is required by IEC [1, 2]. The simulation is performed with a bin width of 4 m/s which is not detailed enough for a design situation, but sufficient to identify the differences in the aerodynamic models. In case of the fault event, rotor blade 3 pitches towards stall at -8 deg/s and the blades 1 and 2 pitch towards feather at +8 deg/s as shown in Fig. 12. The fault event starts at 60s.

Figure 13 shows the development of the electric power as predicted with BEM and the lifting-line FVM. One can see a very good agreement between both aerodynamic models. The calculated

deflections of the rotor blades in out-of-plane direction derived from DLC 2.1 are given in Table 2. Table 2 shows that the out-of-plane deflection calculated with the lifting-line FVM approach is smaller for the rotor blades that are pitched towards feather. For the rotor blade that pitches towards stall, a slightly larger deflection is predicted. A similar result was already shown in Chapter 3 and its relevance for the design process is now confirmed.

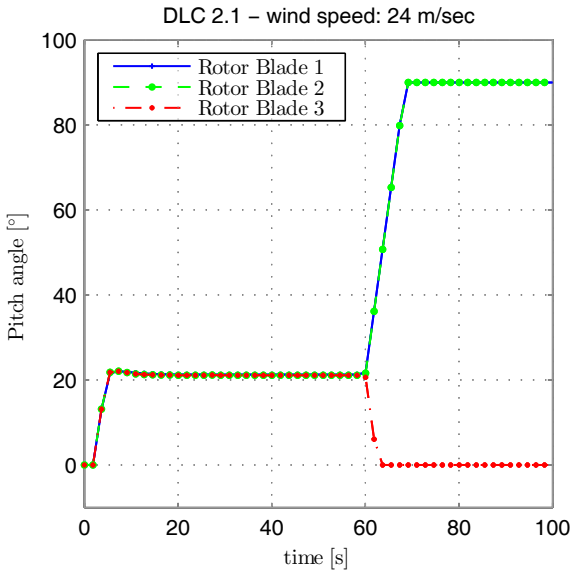

Fig. 12: Pitch angle over time for DLC 2.1

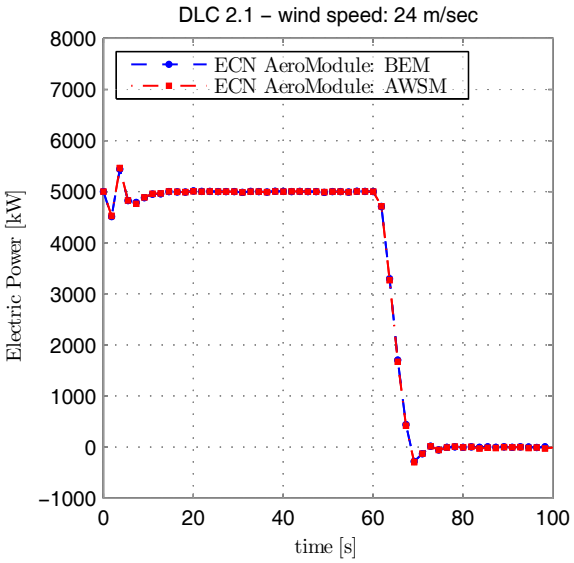

Fig. 13: Power predicted by BEM and AWSM

Table 2: OoP-deflections calculated with BEM and AWSM for DLC 2.1

		aerodynamic method	wind speed	deflection	
out-of-plane deflection blade 1		BEM	16	-3.27	m
	minimum	AWSM	16	-3.38	m
		difference		**3.4%**	-
		BEM	12	4.91	m
	maximum	AWSM	12	4.74	m
		difference		**-3.5%**	-
out-of-plane deflection blade 2		BEM	24	-3.82	m
	minimum	AWSM	24	-3.83	m
		difference		**0.3%**	-
		BEM	12	4.91	m
	maximum	AWSM	12	4.73	m
		difference		**-3.6%**	-
out-of-plane deflection blade 3		BEM	24	-0.58	m
	minimum	AWSM	24	-0.44	m
		difference		**-24.6%**	-
		BEM	24	7.25	m
	maximum	AWSM	24	7.30	m
		difference		**0.7%**	-

4.2. IEC DLC 1.4 Extreme coherent gust with direction change

The turbine is in power production mode when an extreme coherent gust [1] occurs with a simultaneous change of the wind direction. The situation has to be simulated for the rated wind speed v_r and the wind speeds of v_r+2m/s and v_r-2m/s. The direction change has to be considered with both a positive and a negative initial yaw misalignment of ±20 deg, which results in a number of 6 simulations in total.

Figure 14 shows the change in the wind speed and the direction change. Figure 15 illustrates the electric power output as predicted with BEM and AWSM for an initial wind speed of 12m/s.

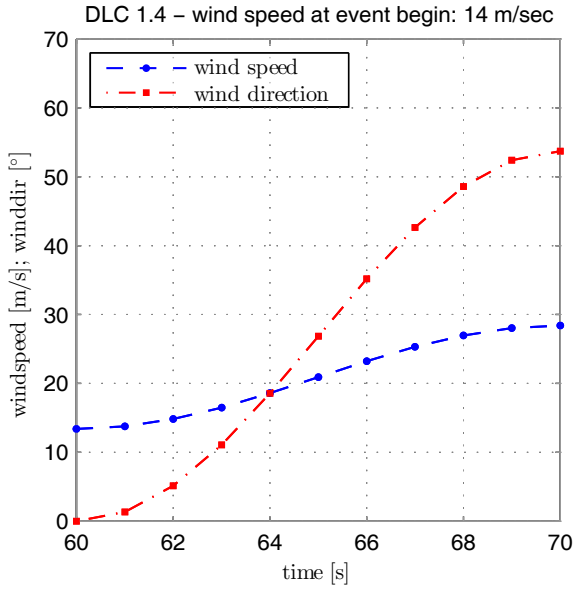

Fig. 14: Wind speed and direction for DLC1.4

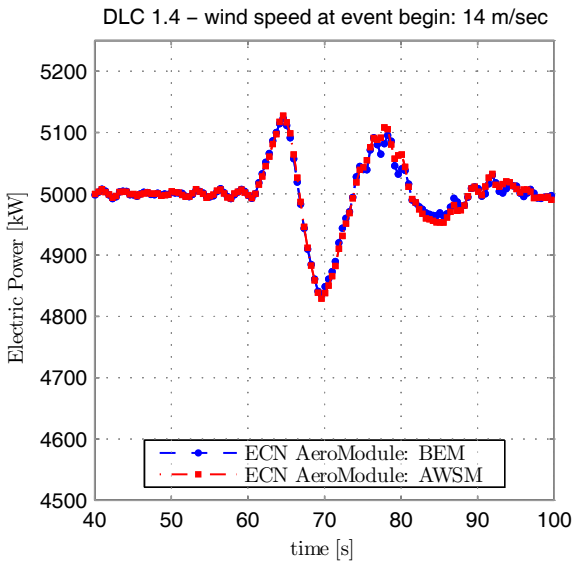

Fig.15: Power predicted by BEM and AWSM

Table 3: Loads and blade deflections calculated with BEM and AWSM

		aerodyn. method	wind field	deflection	
out-of-plane deflection B1	min	BEM	ECD-r+2	-0.98	m
		AWSM	ECD+r+2	-0.96	m
		difference		**-1.3%**	-
	max	BEM	ECD+r	8.63	m
		AWSM	ECD+r	8.35	m
		difference		**-3.3%**	-
out-of-plane deflection B2	min	BEM	ECD-r+2	-2.26	m
		AWSM	ECD-r+2	-2.18	m
		difference		**-3.2%**	-
	max	BEM	ECD+r	8.02	m
		AWSM	ECD+r	7.71	m
		difference		**-3.9%**	-
out-of-plane deflection B3	min	BEM	ECD-r+2	-1.92	m
		AWSM	ECD-r+2	-1.88	m
		difference		**-2.1%**	-
	max	BEM	ECD+r	8.58	m
		AWSM	ECD+r	8.23	m
		difference		**-4.1%**	-

		aerodyn. method	wind field	moment	
tower base moment side-side	min	BEM	ECD+r+20	-8639	kNm
		AWSM	ECD+r+20	-8579	kNm
		difference		**-0.7%**	-
	max	BEM	ECD-r+20	18181	kNm
		AWSM	ECD-r+20	18347	kNm
		difference		**0.9%**	-
tower base moment fore-aft	min	BEM	ECD+r	-6081	kNm
		AWSM	ECD+r	-5569	kNm
		difference		**-8.4%**	-
	max	BEM	ECD+r	89226	kNm
		AWSM	ECD+r	85348	kNm
		difference		**-4.3%**	-
tower base torsion	min	BEM	ECD-r	-5614	kNm
		AWSM	ECD-r	-5941	kNm
		difference		**5.8%**	-
	max	BEM	ECD+r	6252	kNm
		AWSM	ECD+r	6461	kNm
		difference		**3.3%**	-

Table 3 shows the out-of-plane deflection for the three rotor blades. The deflection as predicted with the lifting-line FVM is smaller compared to BEM. The difference between 1% and 4% shows that the BEM results are conservative and there is optimization potential.

Table 3 also shows the overturning moments for the tower base. The tower base loads differ between the determined aerodynamic approaches. It can be concluded that especially the predicted maximum of the fore-aft moment by AWSM is smaller. Nevertheless, the torsional moment is predicted to be higher compared to BEM. This shows that there are situations where the BEM approach underestimates relevant loads. Such inaccuracy has to be covered by the applied safety factors.

5. Conclusion

The advantages of the lifting-line free vortex wake method have been demonstrated for aerodynamic situations that are relevant in the design process and sensitive for the aerodynamic modeling. The influence of blades that are deflected out of the rotor plane has been analyzed, but the differences of the prediction of such a situation in case of a rigid turbine with both aerodynamic models is of academic interest only and has no significance for the design process. The situations with a non-uniform axial induction over the azimuth angle within the rotor plane can be considered much more exact with the lifting-line free vortex wake approach as compared to BEM. This could be verified for a yawed rotor and for a pitch asymmetry situation.

The relevance of the aerodynamic modeling for the design load cases could be verified as well. The load cases IEC DLC 1.4, the occurrence of an extreme coherent gust with direction change, and the IEC DLC 2.1, a fault in the pitch system, have been simulated and the ultimate loads and blade deflections have been analyzed. The relevant targets that are simulated using the lifting-line free vortex wake approach differ up to 5% in contrast to the ones calculated with the blade element momentum theory. For many targets the loads and blade deflections are lower when computed with the lifting-line free vortex method. This indicates the possibility to further optimize the design of wind turbines using this approach as soon as the accuracy of the FVM is proven with measurements.

References

[1] IEC 61400-1: ”Wind turbine generator systems - Part 1: Design requirements“, 3rd edition, August 2005.
[2] Germanischer Lloyd: “Guideline for the Certification of Wind Turbines“, edition 2010.
[3] K. Boorsma, F.Grasso: “ECN AeroModule Users Manual v185”, ECN, August 2012.
[4] A. van Garrel: “Development of a wind turbine aerodynamics simulation module”, TR ECN-C–03-079, ECN, 2003.
[5] D. Simms et al: “Unsteady aerodynamics experiment phases II-IV test configurations and available data campaigns”, TR NREL/TP-500-25950, NREL, 1999.
[6] J.G. Schepers et al: “Model experiments in controlled conditions”, ECN-E–07-042, ECN 2007.
[7] D. Matha, S. Hauptmann, T. Hecquet, M. Kühn: “Methodology and results of loads analysis of wind turbines with advanced aeroelastic multi-body simulation”, DEWEK, Bremen, 2010.
[8] L. Prandtl: “Vier Abhandlungen zur Hydrodynamik und Aerodynamik”, Göttingen, 1927.
[9] J.G. Schepers, L.J. Vermeer: “Een engineering model voor scheefstand op basis van windtunnelmetingen”, TR ECN-CX–98-070, ECN, 1998.
[10] J.G. Schepers: “An engineering model for yawed conditions, developed on basis of wind tunnel measurements”, Technical Report AIAA-1999-0039, AIAA, 1999.
[11] H. Snel, J.G. Schepers: “Joint investigation of dynamic inflow effects and implementation of an engineering model”, Technical Report ECN-C–94-107, ECN, 1994.
[12] B.O.G. Montgomerie et al: “Threedimensional effects in stall”,TR ECN-C–96-079, ECN, 1996.
[13] H. Snel: “Heuristic modelling of dynamic stall characteristics”, EWEC, Dublin, 1997.
[14] T. Theodorsen: “General theory of aerodynamic instability and the mechanism of flutter” Technical Report NACA Report 496, NACA, 1935.

[15] H. Snel: “Application of a modified Theodorsen model to the estimation of aerodynamic forces and aeroelastic stability”, ECN-RX–04-120, ECN, EWEA, London, 2004.
[16] S. Hauptmann et al: “Consideration of aerodynamic effects of blade rotation as computed with URANS in load simulations with BEM”, EWEA, Copenhagen, 2012.
[17] M.O.L. Hansen: “Extraction of lift, drag and angle of attack from computed 3-D viscous flow around a rotating blade” Proc. of EWEC 499–502, 1997.
[18] Schepers J.G et al: “Results from mexnext: Analysis of detailed aerodynamic measurements on a 4.5 m diameter rotor placed in the large german dutch wind tunnel DNW” Technical Report ECN-M– 11-034, ECN, April 2011. EWEA, Brussels, 2011.
[19] E. Branlard et al: “An improved tip-loss correction based on vortex code results”, EWEA, Copenhagen, 2012.
[20] Glauert, H.: “The Analysis of Experimental Results in the Windmill Brake and Vortex Ring State of an Airscrew”, Technical Report ARC R&M No. 1023, 1926
[21] Glauert, H.: “A General Theory of the Autogyro”. Technical Report ARC R&M No.1111, 1926